Article

Fabrication of the Metal-Organic Framework Membrane with Excellent Adsorption Properties for Paraben Based on Micro Fibrillated Cellulose

LI Jingkang[1], JIANG Yanxiao[2], YANG Jukun[1], SUN Ying[1], MA Pinyi[1]✉ and SONG Daqian[1]✉

Received December 30, 2021
Accepted March 12, 2022

A kind of novel environmental-friendly composite absorbent material was designed and prepared in this paper. Nanoscale metal-organic frameworks(MOFs) were embedded in the skeleton of cotton micro fibrillated cellulose. By scanning electron microscope(SEM), we observed that a large number of MOFs were attached to the cellulose skeleton. In addition, under the condition of 1800 r/min vortex, the structure of the composite material was stable and was not easily damaged by external forces. The water contact angle test showed that the composite material had excellent hydrophilicity and could be used for the adsorption of pollutants. Then, the material was characterized by energy dispersive X-ray spectroscopy(EDX), X-ray diffraction(XRD), Fourier transform infrared spectroscopy(FTIR) and BET adsorption. Through verification, the material had very stable reusability(n=10). The composite material was applied to the solid phase extraction of water samples, such as rain water, toning water and fruit juice, and was quantitatively analyzed by high performance liquid chromatography(HPLC)-UV. This method was then applied to the extraction of four parabens(methyl-, ethyl-, propyl-, and butyl-paraben) from real samples, yielding limits of detection(LODs) of 0.29—0.58 ng/mL. The linear range was 2—500 ng/mL. The inter-day and intra-day recoveries were 90.7%—106.0% and 87.1%—109.3%, respectively(relative standard deviation<10.8%).

Keywords Micro fibrillated cellulose; Metal-organic framework; Paraben; Solid phase extraction

1 Introduction

p-Hydroxybenzoic acid demonstrates antimicrobial activities (when used alone or in combination), and this effective antimicrobial agent has found widespread application[1]. However, recent reports suggest that exposure to parabens may regulate or disrupt the endocrine system, which may have harmful consequences for human health[2]. In particular, parabens are endocrine disruptors with low estrogen activity, and thus there is a potential risk of breast cancer in women and a possible adverse effect on male infertility[3]. In this paper, four common paraben parabens, methyl-paraben(MP), ethyl-paraben(EP), propyl-paraben(PP) and butyl-paraben(BP) were studied.

Metal-organic framework(MOF) materials have been demonstrated to be an excellent adsorption material for use in the enrichment and extraction of organic small molecule pollutants[4,5]. MOFs are a type of porous material composed of metal clusters and organic species[6], and each MOF is characterized by a unique network of holes[7]. In addition, MOFs are considered a promising sample preparation material for use in the field of analytical chemistry[8], and they are increasingly used for the extraction or adsorption removal of various toxic organic substances in the liquid phase[9]. In 2015, Afonso *et al*.[10] used a metal-organic framework, HKUST-1 (Cu), as an effective adsorbent for the eddy-current assisted dispersion micro solid-phase extraction(SPE) of parabens.

When MOF powder is directly used for enrichment and adsorption, centrifugation is often used. High speed centrifugation is required during extraction and elution, and the transfer process is also highly demanding because the loss of solid powder is caused during the transfer process. So the direct use of powdered MOFs for solid phase extraction is complicated. Furthermore, there is an associated loss of adsorbents during the sample pre-treatment process, and this can lead to errors. Now, many people choose to combine various polymers with MOFs to form membrane composites[11]. In 2014, Mao *et al*.[12] combined polyvinylidene fluoride(PVDF) with HKUST-1(Cu) by using a pressure-assisted room temperature growth strategy and prepared continuous and well-developed HKUST-1(Cu) films, which were gas separation. PVDF is extremely hydrophobic, so the membrane is not suitable for water samples. Therefore, some researchers choose cellulose filter paper as a carrier to make a new type of composite material.

Cellulose is an excellent natural adsorbent. Cellulose filter

✉ MA Pinyi
mapinyi@jlu.edu.cn
✉ SONG Daqian
songdq@jlu.edu.cn
1. College of Chemistry, Jilin Province Research Center for Engineering and Technology of Spectral Analytical Instruments, Jilin University, Changchun 130012, P. R. China;
2. School of Marine Science and Technology, Harbin Institute of Technology at Weihai, Weihai 264209, P. R. China

https://doi.org/10.1007/s40242-022-1511-5

paper demonstrates both an excellent liquid adsorption capacity and water permeability. However, ordinary cellulose filter paper is not selective, and it cannot be used to selectively extract small molecular organic matter, such as *p*-hydroxybenzoate. In 2019, Jiang *et al*.[13] used chitosan as the adhesive to coat the surface of filter paper with metal organic skeleton MIL-101(Cl) for thin film microextraction of triazine herbicides. However, when chitosan is used as the adhesive, there is a significant loss of loaded MOFs under the condition of high-speed vortex.

In the present study, micro fibrillated cellulose(MFC) was combined with MOFs, and the MOFs were inserted into the skeleton of MFC, and then a new composite material for the separation and enrichment was designed and prepared. Cellulose itself is an environmentally friendly material that can be easily degraded. Moreover, the experimental data show that the composite can be recycled more than 10 times and could achieve good reusing. The material was used to extract *p*-hydroxybenzoate, and then quantitative analysis was performed by high performance liquid chromatography (HPLC). In comparison with traditional extraction methods, the method reported in this study is extremely convenient and has higher relative recoveries(RRs%)[14,15]. The relative recovery(RR, %) was obtained as Equation (1):

$$\mathrm{RR}(\%) = \frac{c_i}{c_0} \times 100\% \quad (1)$$

where c_i and c_0 are the concentrations of analyte in the sample measured experimentally, and the theoretical concentration of analyte in the sample calculated by linear equation, respectively.

2 Experimental

2.1 Reagents and Instruments

Reagent and instrument information can be found in the Electronic Supplementary Material of this paper(Table S1).

2.2 Preparation of MOF/MFC Membrane

MIL-68(Al) was synthesized following the reported method[16], and the synthesis steps can be found in the Electronic Supplementary Material of this paper. The two-dimensional membrane was prepared by vacuum filtration according to the previously reported method[17]. The detailed preparation process was described in the Electronic Supplementary Material of this paper(Fig.S1). As shown in Fig.1, the celluloses individually form colloidally stable suspensions but assemble into covalently crosslinked clusters with entrapped MOFs when mixed together. The MOFs-cellulose interaction is mainly due to the physical entanglement and van der Waals interaction between MOFs and cellulose[18]. As a result, MOFs attach to the cellulose skeleton due to van der Waals forces. When MFC skeletons crosslinked and physically entangled, MOFs are embedded to them. Then we succeeded in getting MOF/MFC membrane(MMm).

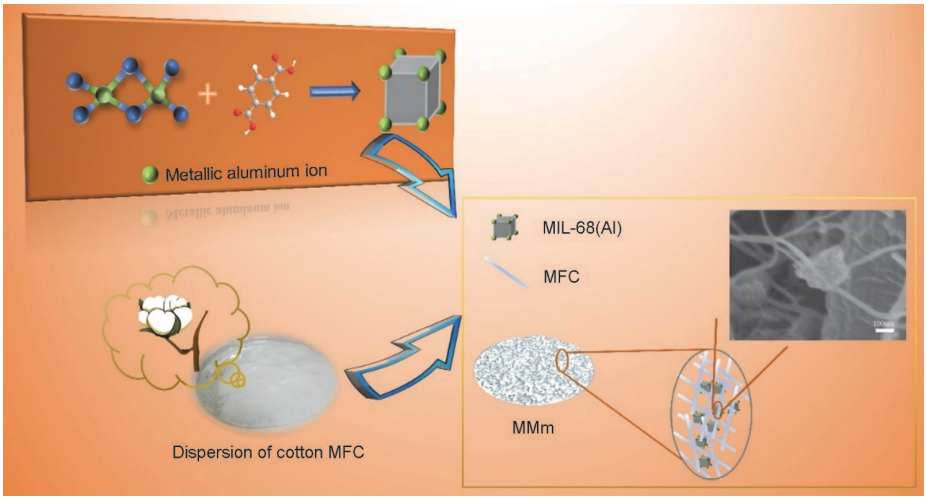

Fig.1 Flow chart of MMm preparation

2.3 Adsorption Experiments

2.3.1 SPE Procedure and HPLC Analysis

The sample preparation and extraction procedures are shown in Fig.S2(see the Electronic Supplementary Material of this paper). Briefly, 5 mL of spiked water(pH=5, 0% salt concentration) was transferred into a centrifuge tube. Next, an MIL-68(Al)/MFC membrane was placed in the centrifuge tube, and the tube was then vortexed for 12 min to adsorb the target. After adsorption, the liquid was decanted from the centrifuge tube. The membrane was then left stand for approximately

https://doi.org/10.1007/s40242-022-1511-5

2 min without the lid to evaporate the moisture from the membrane. Next, 3 mL of acetonitrile was added to the centrifuge tube, and the tube was vortexed for 15 min to desorb the target. The acetonitrile solution containing the target analyte was then dried by N_2 blowing at 318 K. Finally, the target was re-dissolved in 100 μL of acetonitrile, and then filtered through a 0.22 μm nylon membrane for HPLC analysis.

2.3.2 Static Adsorption Experiment

In order to better explore the adsorption properties of the material, some kinetic models are used to assist the explanation. Isothermal adsorption experiments were performed under the following conditions: at 298 K, MMm(or blank MFC) was added to EP samples at varying concentrations(c_i, mg/L) ranging from 10 mg/L to 200 mg/L. It was then oscillated overnight at 250 r/min. The shape and phase of MMm are stable and will not affect the liquid transfer and subsequent tests. Finally, the equilibrium concentration of EP(c_e, mg/L) was determined by UV-Vis spectrophotometer at 257 nm. The equilibrium binding ability(Q_e, mg/g) of EP on MMm can be calculated as Equation (2):

$$Q_e = \frac{c_i - c_e}{m} V \quad (2)$$

where m is the mass of MOFs loaded in MMm, and V is the volume of sample liquid. Isothermal adsorption experiments were performed under the following conditions: at 298 K, MMm was added to EP samples. It was then oscillated at varying time(c_t, mg/L) ranging from 3 min to 600 min at 250 r/min. Finally, the concentration of EP was determined on a UV-Vis spectrophotometer at 257 nm. The temporal adsorption capacity(Q_t, mg/g) was determined according to Equation (3):

$$Q_t = \frac{c_i - c_t}{m} V \quad (3)$$

3 Results and Discussion

3.1 Characterization

Powder X-ray diffraction(XRD) analysis was conducted on a D8 ADVANCE X-ray diffractometer(BRUKER, Germany) using Cu $K\alpha$ radiation(λ=0.15406 nm). An XRD diffractogram was recorded within the 2θ range of 3°—90°. XRD patterns for the three different MOFs are demonstrated in Fig.S3(A)(see the Electronic Supplementary Material of this paper). The characteristic peaks are in accordance with previous reports[19—21]. In addition, N_2 physisorption isotherms of MIL-68(Al) were measured using a surface area and pore analyzer instrument(Belsorp max, Microtrac BEL, Japan). The permanent porosity of MIL-68(Al) was evaluated in a N_2 adsorption isotherm experiment at 77 K. The results are shown in Fig.S3(B) and (C)(see the Electronic Supplementary Material of this paper). Moreover, Fourier transform infared spectroscopy(FTIR) was also carried out on the three synthesized MOFs(Fig.S4, see the Electronic Supplementary Material of this paper). In FTIR spectrum, strong peaks around 3400 cm^{-1} were ascribed to the stretching band of —OH groups. Peaks at 1650—1430 cm^{-1} were corresponded to the COO— stretching vibration and C—C stretching vibration of benzene, which demonstrated the presence of the carboxylate linker of MOFs[22]. As a large number of benzene ring structures are still retained in MOFs, it is very likely to generate π-π interaction with the adsorbed substance, forming chemisorption[23].

All synthesis procedures can be found in the Electronic Supplementary Material of this paper. After MOF synthesis, we characterized the three different synthetic MOFs by scanning electron microscopy(SEM). The element distribution of the three MOFs was analyzed by energy dispersive X-ray spectroscopy(EDX)(Figs.S5—S7, see the Electronic Supplementary Material of this paper). As shown in Fig.2, MIL-101(Cr) demonstrated the smallest particle size, followed by MIL-68(Al). In contrast, HKUST-1(Cu) demonstrated a much larger particle size than the other two MOFs. According to the above test results, we successfully synthesized three MOFs. Next, we combined each of the three MOFs with cellulose paper film to generate three different MMms.

The characterization by SEM is shown in Fig.2. In Fig.2(A)—(C), it shows the structural characterization of three kinds of MOFs. In Fig.2(D), the skeleton structure of cellulose paper can be clearly observed, and many small particles of MOFs can be observed attached to the skeleton. It is clear from Fig.2(E) that MOFs are indeed embedded in the skeletons of the MFC. Then we also verified the hydrophilicity of the material, and if the water contact angle is less than 60°, the material has good hydrophilicity. In Fig.S8(see the Electronic Supplementary Material of this paper), we can see that the blank MFC membrane itself has a good hydrophilicity. Combining it with MIL-68(Al), an extremely hydrophilic material, the resulting composite membrane material is also extremely hydrophilic. It would be widely used in water samples. As shown in Fig.S9(C)—(E)(see the Electronic Supplementary Material of this paper), during the whole process of material preparation, it can be judged from the clarity of filtrate that this method has almost no material loss. Then the structural stability of the membrane was also tested by mechanical tests in high-speed vortex and ultrasonic environments. As can be seen from Fig.S9(A), c-MMM still exists stably in water after more than 600 min of 1800 r/min vortex. When it is put into the water sample, there is no obvious change in the ultrasound between 0—30 min. When the ultrasonic time is too long, flocs will be seen in the water,

https://doi.org/10.1007/s40242-022-1511-5

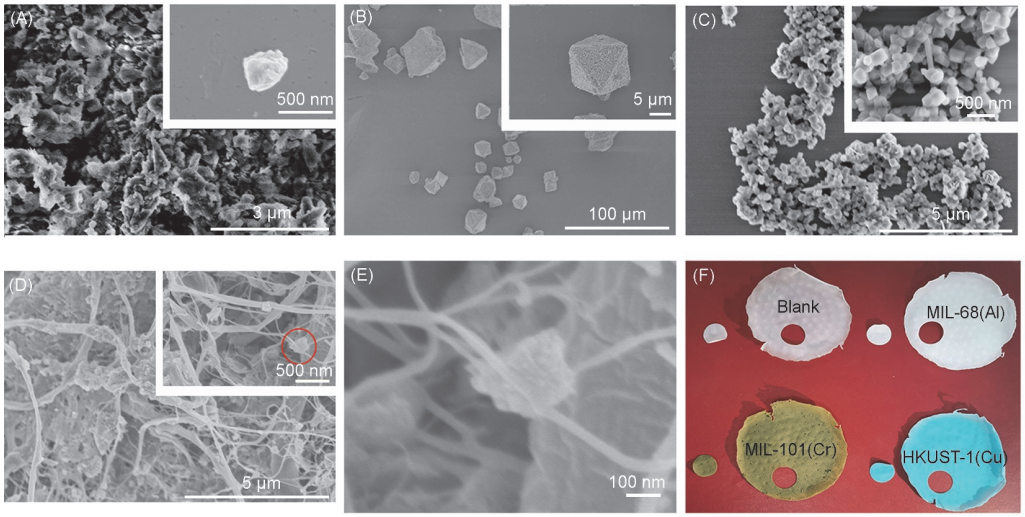

Fig.2 SEM characterization of materials

(A) MIL-68(Al); (B) HKUST-1(Cu); (C) MIL-101(Cr); (D) MIL-68(Al)/MFC; (E) magnified image of the part marked red in the inset of (D); (F) blank MFC, MIL-68(Al)/MFC, HKUST-1(Cu)/MFC, and MIL-101(Cr)/MFC. Insets: (A) a single MIL-68(Al) at higher magnification; (B) a single HKUST-1(Cu) at higher magnification; (C) MIL-101(Cr) at higher magnification; (D) MIL-68(Al)/MFC at higher magnification.

which proves that the structure of the material will have a structural collapse in the long-term ultrasonic environment.

3.2 Optimization of the Proposed Procedure

3.2.1 Comparison of Different MMms

Three MMms were prepared from three different MOFs, HKUST-1(Cu), MIL-101(Cr) and MIL-68(Al). We then assessed the performance of these three MMms during experiments involving the adsorption of parabens. As shown in Fig.3(A), the three MFC membranes produced using the new materials designed in this study all demonstrate paraben adsorption capabilities. Of the three MMms assessed, the MIL-68(Al)/MFC membrane demonstrated the best adsorption. Therefore, in subsequent experiments, the MIL-68(Al)/MFC membrane was used as an extractant to develop and design a new solid-phase extraction method. This material was then applied to the experimental determination of *p*-hydroxybenzoate. Under the experimental conditions described here, the relative recoveries(RRs%) were between 87.1% and 109.3%.

Because the metal-organic skeleton of the material plays a key role in adsorption, we first evaluated the loading capacity of MOFs. Initially, as the amount of coating increases, the RRs% also gradually increase[Fig.3(B)]. However, the RRs% then plateau at high amounts of coating[Fig.3(B)]. The highest RR% was achieved at a load of 125 mg. After statistical calculation, the mass of MOFs on the clipped-MMm(c-MMm) is about 10 mg(Fig.S10, see the Electronic Supplementary Material of this paper). Therefore, to optimize and save on raw materials, 125 mg was selected as the load mass for MOFs in subsequent experiments.

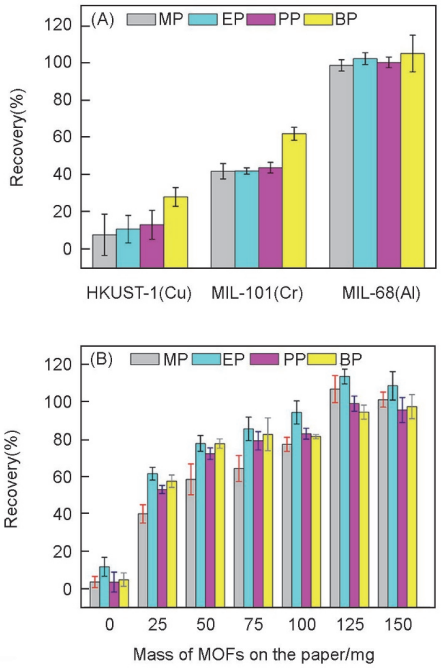

Fig.3 Optimization of preparation conditions

(A) Bar graph showing the optimization of MOFs type; (B) bar graph showing the optimization of adsorption mass of MOFs on the paper.

3.2.2 Effect of Sample pH

The pH of the applied sample plays an important role in the extraction of targets. In particular, pH can affect both the charge and density of the species on the adsorbent surface, as well as the forms of the target analytes. To test the extraction performance of c-MMms under different pH conditions, we compared and analyzed six water samples at different pH values. As shown in Fig.4(A), pH had a minimal effect on RR% over the pH range of 3—8(although RR% was slightly higher at pH=5). In contrast, the RR% progressively decreased over

https://doi.org/10.1007/s40242-022-1511-5

the pH range of 8—11. According to previous studies[24], the structures of MOFs are stable in acidic and neutral solutions. However, MOFs synthesized with terephthalic acid as a ligand can decompose as the alkalinity gradually increases(and can even completely decompose in the case of strong alkalinity). Therefore, we chose pH=5 as the pH of the sample solution in subsequent experiments.

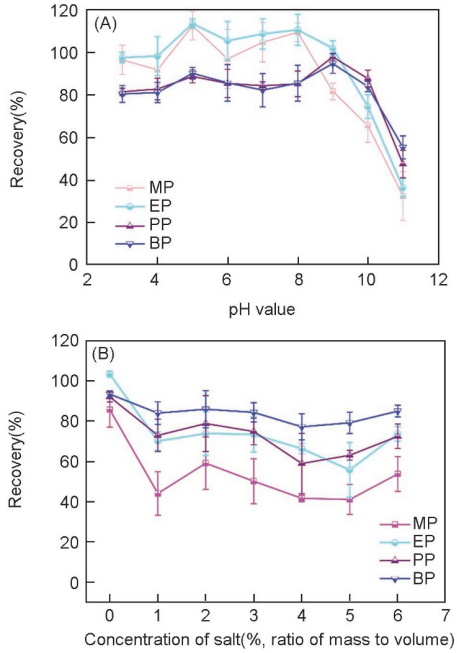

Fig.4 Optimization of experimental conditions

(A) Optimization of sample pH; (B) optimization of salt concentration.

3.2.3 Effects of Salt Concentration on Extraction

The addition of NaCl generally decreases the solubility of the target analyte in the sample solution due to the salting-out effect, which consequently affects the extraction efficiency[25]. To evaluate possible interference with the assay by the salting-out effect, the extraction RR% was studied under the conditions of 0—6%(ratio of mass to volume) NaCl(with other parameters unchanged). As shown in Fig.4(B), the extraction recoveries of all the parabens are significantly reduced in the presence of NaCl(in comparison to extraction recoveries in the absence of NaCl). The most likely explanation is that the viscosity of the solution increased with the increase in salt concentration, which is unfavorable for the diffusion of analytes. Thus, NaCl was not added in subsequent experiments.

3.2.4 Vortex Adsorption Time

The effect of vortex oscillation time on extraction RR% was investigated by varying vortex assisted extraction between 1 and 18 min. As shown in Fig.5(A), the RR% initially increases gradually from 1 min to 12 min, and remains relatively stable after 12 min. Therefore, a 12-min vortex adsorption time was used in subsequent experiments.

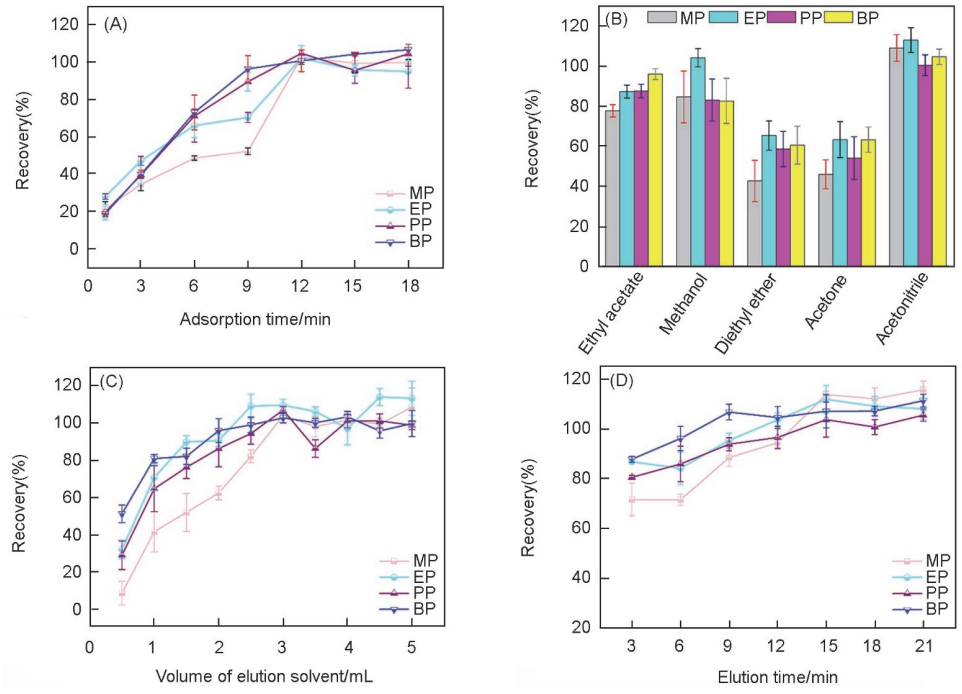

Fig.5 Optimization of experimental conditions

(A) Optimization of adsorption time; (B) optimization of elution solvent; (C) optimization of elution solvent volume; (D) optimization of elution time.

https://doi.org/10.1007/s40242-022-1511-5

3.2.5 Effects of Desorption Condition

In addition to the optimization of experimental conditions during the adsorption stage, we also investigated the desorption process. The type of desorption solvent, the eddy time of desorption, and the volume of the adsorption solvent were all observed to have a marked influence on the experimental results. Therefore, we subsequently performed an optimization of the desorption process. First, five solvents with different polarities were selected for comparison. As shown in Fig.5(B), acetonitrile demonstrates the highest efficacy. The extraction recoveries for the five solvents decreased as follows: acetonitrile>methanol and ethyl acetate>acetone and ethyl. Therefore, we subsequently used acetonitrile as our desorption solvent in subsequent experiments.

Next, we optimized the volume of the desorption solvent, assessing extraction recoveries from volumes in the 0.5—5 mL range. As shown in Fig.5(C), while the extraction RR% increases gradually as the volume increases from 0.5 mL to 3 mL, there is no significant change at higher volumes. To optimize RR%, provide cost savings and reduce organic solvent waste, 3 mL was selected as the volume of desorption solvent in subsequent experiments.

The duration of vortex oscillation is an important factor in sample pretreatment, demonstrating a direct effect on extraction RR%. To investigate the effects of duration of vortex oscillation on extraction RR%, the desorption time was varied from 3 min to 21 min. As shown in Fig.5(D), the extraction RR% increases gradually over the 3 min to 15 min range, and then plateaus at higher desorption time. Therefore, the desorption time was set at 15 min in subsequent experiments.

3.3 Various Properties of c-MMms

3.3.1 Adsorption Properties of c-MMms

In order to test the adsorption properties of c-MMm, static adsorption equilibrium experiments in the initial concentration range of 1—200 mg/L were performed. As can be seen from Fig.6(A), adsorption performance of c-MMm increases with the increase of sample concentration. With the increase of sample concentration, the adsorption sites on c-MMm eventually reach saturation and the adsorption capacity reaches the upper limit. Results show that c-MMm has good adsorption performance, because MIL-68(Al) loaded on MFC has a good adsorption effect on EP. The curve was linearly fitted(R^2=0.99). The optimal fitting curves of c-MMm have been illustrated in Fig.6.

In addition to the material adsorption performance test, Langmuir and Freundlich models were used to fitting the experimental result. Detailed mathematical models and parameter information can be seen in Table S2(see the Electronic Supplementary Material of this paper). According to Fig.6(B) and (C), the fitting situation of Langmuir(R^2=0.982) and Freundlich(R^2=0.948) could suggest that the isothermal adsorption of c-MMms for EP was not only monolayer adsorption, but also heterogeneous and multilayer binding[26,27].

The adsorption efficiency of c-MMm for EP was determined by kinetic experiments. As can be seen from Fig.6(D), the adsorption capacity of c-MMm for EP increases with time increasing. MIL-68(Al) loaded on MFC is a

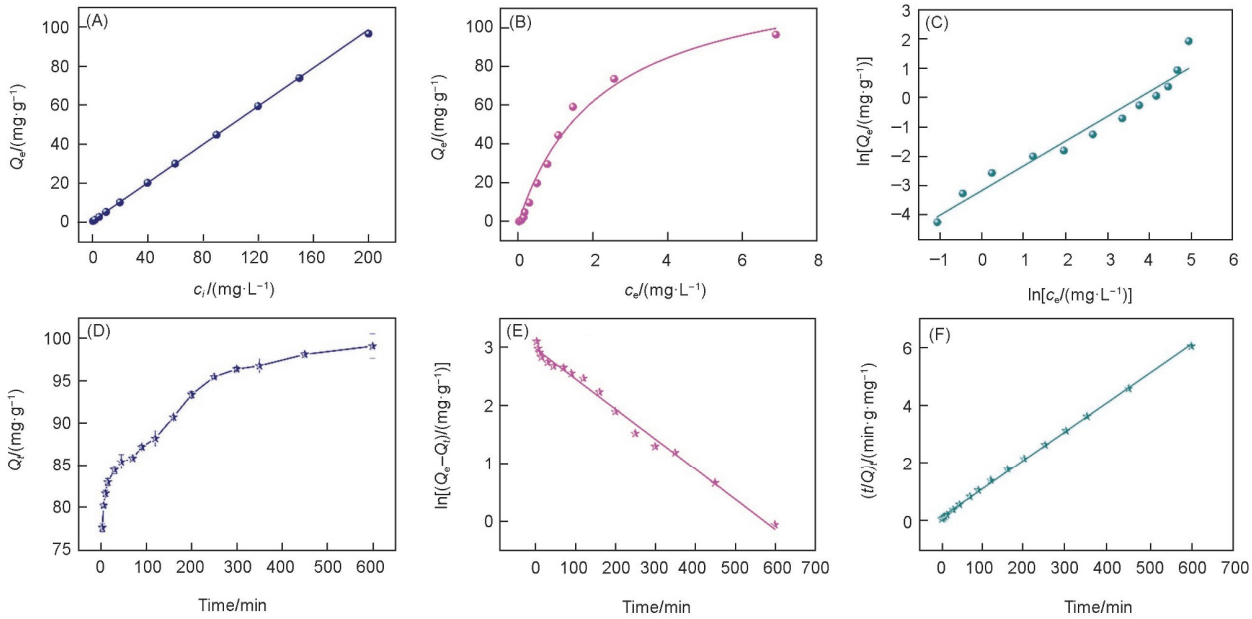

Fig.6 Adsorption isotherms

(A) Adsorption performance of c-MMm; (B) Langmuir model; (C) Freundlich model, (D) adsorption kinetics: (E) pseudo-first-order model; (F) pseudo-second-order model.

https://doi.org/10.1007/s40242-022-1511-5

nanoscale porous material, which facilitates the transfer and diffusion of substances with specific sizes, such as parabens.

The pseudo-first-order model and pseudo-second-order model were used to describe and analyze the results of the dynamics. The equation and parameters are shown in Table S3 (see the Electronic Supplementary Material of this paper). As shown in Fig.6(E) and (F), after using pseudo-first-order model fitting and pseudo-second-order model fitting, the fitting results are based on pseudo-first-order model(k_1=0.0052, R^2=0.991). According to k_1, when static adsorption is used, the rate of adsorption is low. In the SPE pretreatment, vortex-assisted extraction is added, which greatly improves the adsorption rate of the experiment. Meanwhile, the material does not disintegrate under vortex oscillations. The fitting results based on pseudo-second-order model(R^2=0.979) are obtained. The adsorption process of c-MMm for EP contains not only adsorption in the physical structure, but also chemical adsorption[28]. In addition to adsorption, due to aperture size, electrostatic force and usual hydrogen bond, the other adsorption interaction force is a powerful chemical adsorption interaction. It also further verified the conclusion of the previous characterization. There is chemisorption(π-π interaction) between MOFs and *p*-hydroxybenzoic acid esters.

3.3.2 Reusability of c-MMms

To test the additional advantages of our novel material, we performed experiments that investigated c-MMms reusability. Fig.S11(see the Electronic Supplementary Material of this paper) demonstrates the data obtained after re-using c-MMms 10 times (number of parallel samples=3). The results reveal that the performance of the material did not change markedly after 10 times of use, indicating that the material has good reusability.

3.4 Evaluation of Extraction Method

Under the above-optimized conditions, the analytical performance of the V-SPE/HPLC method was assessed on the basis of a series of quantitative indicators. These included the linear ranges(LRs), correlation coefficients, limits of detection (LODs), and values of inter-day and intra-day precision (Table 1). The linear regression equation and correlation coefficient of the analytes are reported in Table 1. In the concentration range of 2—500 ng/mL, all four *p*-hydroxybenzoates demonstrated a good linear relationship($r \geqslant 0.9985$). For all the *p*-hydroxybenzoates, the LODs(signal-to-noise ratio S/N=3) were 0.29—0.58 ng/mL. Reproducibility was assessed by measuring intra-day and inter-day precision at two different concentrations over one working day and six consecutive days, respectively. As shown in Table 1, the intra-day and inter-day RRs% for the four *p*-hydroxybenzoate samples were 87.1%—109.3% and 90.7%—106.0%, respectively. The associated RSDs of intra-day and inter-day precision were 2.6%—10.8% and 3.5%—8.2%, respectively. The above data demonstrate the excellent precision obtained using this method.

Table 1 Analytical performance of the present method

Analyte	Linear range/ (ng·mL^{-1})	Regression equation	Correlation coefficient(r)	Spiked amount/ (ng·mL^{-1})	Intra-day(n=6)		Inter-day(n=6)		LOD/(ng·mL^{-1})
					RR(%)	RSD(%)	RR(%)	RSD(%)	
Methylparaben	2.0—500.0	y=1113.6x–8944.7	0.9989	40	100.7	3.5	95.0	6.1	0.29
				200	87.1	3.8	97.7	5.9	
Ethylparaben	2.0—500.0	y=1159.0x+4527.8	0.9985	40	97.6	10.6	102.2	4.5	0.45
				200	101.0	2.0	106.0	3.6	
Propylparaben	2.0—500.0	y=1566.2x–10193.8	0.9987	40	109.3	9.2	100.3	5.8	0.50
				200	90.0	4.8	90.7	7.0	
Butylparaben	2.0—500.0	y=1486.5x–7837.0	0.9993	40	102.7	7.0	95.5	3.5	0.58
				200	97.1	3.3	92.8	6.3	

3.5 Application of Real Samples

To evaluate the practicalities of our method, the method was applied to the determination of parabens in five real samples, rainwater, drinking water, tap water, juice and lotion. The juice was first processed by high speed centrifugation, and the supernatant was recovered for subsequent experiments. All experiments were performed as described in Section **2.3.1**. The final results are reported in Table S4(see the Electronic Supplementary Material of this paper). The RRs% values of all the parabens ranged from 83.7% to 105.0%(with RSDs less than 13.1%).

3.6 Comparison of Our Method with Published Methods

In the present study, a new extraction method was proposed and optimized. A comparison of results previously reported, which used different methods with the results obtained using our novel method is shown in Table 2[10,20,29—31]. In comparison with previous methods, the simple vortex-assisted extraction

Table 2 Comparison of the presented method with other reported methods

Matrix	Analyte	Extraction method	Extraction time/min	Analytical technique	RR(%)	RSD(%)	LOD/(ng·mL^{-1})	Ref.
Human breast milk	MP, EP, PP	μSPE[a]	—	HPLC-UV	87.2—104.4	⩽8.9	3.0—5.0	[29]
Cosmetic, river water, waste water	MP, EP, PP	FPSE[b]	40	HPLC-PDA[g]	71.4—102.4	⩽3.8	2.8—3.0	[30]
Vegetable oil	MP, EP, PP, BP	MEPS[c]	11	HPLC-MS/MS	72.2—119.7	⩽14.0	0.6—1.4	[20]
Environmental water, cosmetic cream, urine	MP, EP, PP, iPP	VA-D-mSPE[d]	33	HPLC-DAD[h]	61.3—101.0	⩽15.0	1.5—2.6	[10]
Water	EP, PP, BP	EME[e]	40	HPLC-DAD	80.4—103.6	<12.6	0.7—1.2	[31]
Rainwater, drinking water, tap water, juice, lotion	MP, EP, PP, BP	V-SPE[f]	15	HPLC-UV	87.1—109.3	⩽10.8	0.3—0.6	This work

a. Micro solid-phase extraction; *b*. fabric phase sorptive extraction; *c*. microextraction packed syringe; *d*. vortex-assisted dispersive micro solid-phase extraction; *e*. electro-membrane extraction; *f*. vortex-assisted solid-phase extraction; *g*. photodiode array; *h*. diode array detection.

method described in this paper simplifies the traditional SPE procedure while maintaining the original high RRs% and stability. Furthermore, because c-MMm is a kind of environment-friendly material, no additional pollution is introduced when using our novel method for the detection of parabens.

4 Conclusions

In the present study, three kinds of MOF/MFCs were prepared by a simple vacuum filtration method. These materials were characterized by SEM, EDX, XRD, FTIR and the BET adsorption isotherm. The three materials were then used in the sample pre-treatment process. Our experimental results reveal that MIL-68(Al)/MFC demonstrated the best adsorption performance for terephthalate. To experimentally determine paraben levels, an optimized vortex-assisted solid phase extraction(SPE) method was used. The use of thin MMms simplified the solid-liquid separation process, and the whole process was very convenient. Because MIL-68(Al)/MFC can be used as a selective filter membrane, it holds great potential for further development in the future. However, the structure of the material is easy to disintegrate in the environment of long-time ultrasonic treatment. In the future, we will try to further process the material to stabilize its structure so that it can be used in more and more complex environments.

Electronic Supplementary Material

Supplementary material is available in the online version of this article at http://dx.doi.org/10.1007/s40242-022-1511-5.

Acknowledgements

This work was supported by the National Natural Science Foundation of China (Nos.22074052 and 22004046) and the Science and Technology Developing Foundation of Jilin Province of China(No.20200404173YY).

Conflicts of Interest

The authors declare no conflicts of interest.

References

[1] Soni M. G., Carabin I. G., Burdock G. A., *Food Chem. Toxicol.*, **2005**, *43*(7), 985
[2] Darbre P. D., *Best Pract. Res. Clin. Endocrinol. Metab.*, **2006**, *20*(1), 121
[3] Barajas-Salinas A., Ducolomb Y., Betancourt M., Núñez-Macías, E., López A., Barraza J., Quezadas-Fuentes J., Bahena-Ocampo I., Bonilla E., Retana-Márquez S., Casas E., Casillas F., *J. Appl. Toxicol.*, **2021**, *41*(2), 330
[4] Liu C. Y., Chen X. R., Chen H. X., Niu Z., Hirao H., Braunstein P., Lang J. P., *J. Am. Chem. Soc.*, **2020**, *142*, 6690
[5] Liu D., Lang J. P., Abrahams B. F., *J. Am. Chem. Soc.*, **2011**, *133*, 11042
[6] Furukawa H., Cordova K. E., O'Keeffe M., Yaghi O. M., *Science*, **2013**, *341*, 6149
[7] Chen Y. Z., Zhang R., Jiao L., Jiang H. L., *Coord. Chem. Rev.*, **2018**, *362*, 1
[8] Li X., Ma W., Li H., Bai Y., Liu H., *Coord. Chem. Rev.*, **2019**, *397*(18), 1
[9] Ma W., Li X., Bai Y., Liu H., *Trends Anal. Chem.*, **2018**, *109*, 154
[10] Rocío-Bautista P., Martínez-Benito C., Pino V., Pasán, J., Ayala J. H., Ruiz-Pérez C., Afonso A. M., *Talanta*, **2015**, *139*, 13
[11] Lang J. P., Xu Q. F., Yuan R. X., Abrahams B. F., *Angew. Chem. Int. Ed.*, **2004**, *43*, 4741
[12] Mao Y., Li J., Cao W., Ying Y., Sun L., Peng X., *ACS Appl. Mater. Interfaces*, **2014**, *6*(6), 4473
[13] Jiang Y., Ma P., Piao H., Qin Z., Tao S., Sun Y., Wang X., Song D., *Microchim. Acta*, **2019**, *186*, 742
[14] Tartaglia A., Kabir A., Ulusoy S., Sperandio E., Piccolantonio S., Ulusoy H. I., Furton K. G., Locatelli M., *J. Chromatogr. B*, **2019**, *1125*, 121707
[15] Razavi N., Es'haghi Z., *Microchem. J.*, **2019**, *148*, 616
[16] Chen Z., Yu C., Xi J., Tang S., Bao T., Zhang J., *Microchim. Acta*, **2019**, *186*(6), 1
[17] Karim Z., Monti S., Barcaro G., Svedberg A., Ansari M. A., Afrin S., *Environ. Sci. Nano*, **2020**, *7*(10), 2941
[18] Zhu H., Yang X., Cranston E. D., Zhu S., *Adv. Mater.*, **2016**, *28*(35), 7652
[19] Jiang Y., Piao H., Qin Z., Li X., Ma P., Sun Y., Wang X., Song D., *J. Sep. Sci.*, **2019**, *42*(18), 2900
[20] Jiang Y., Qin, Z., Song X., Piao H., Li J., Wang X., Song D., Ma P., Sun Y., *Microchem. J.*, **2020**, *158*, 105200
[21] Wang C., Zhou W., Liao X., Wang X., Chen Z., *Anal. Chim. Acta*, **2018**, *1025*, 124
[22] Ma W., Li J., Li X., Liu H., *J. Hazard. Mater.*, **2022**, *422*, 126839
[23] Yin Y., Shi M., Ren Y., Wang S., Hua M., Lu J., Zhang W., Lv L., *Chem. Eng. J.*, **2020**, *387*, 124196
[24] Zhao X., Liu D., Huang H., Zhang W., Yang Q., Zhong C., *Microporous Mesoporous Mater.*, **2014**, *185*, 72
[25] Rozaini M. N. H., Yahaya N., Saad B., Kamaruzaman S., Hanapi N. S. M., *Talanta*, **2017**, *171*, 242
[26] Piao H., Ma P., Qin Z.. Jiang Y., Sun Y., Wang X., Song D., *Chem. J. Chinese Universities*, **2020**, *41*(2), 228
[27] Cui Y., Lin J., Xu Y., Li Q., Chen Y., Ding L., *Sep. Purif. Technol.*, **2021**, *276*, 119302
[28] Cui Y., He Z., Xu Y., Su Y., Ding L., Li Y., *Chem. Eng. J.*, **2021**, *405*, 126608
[29] Manouchehri M., Seidi S., Rouhollahi A., Noormohammadi H., Shanehsaz M., *Food Chem.*, **2020**, *314*, 126223
[30] Gülle S., Ulusoy H. I., Kabir A., Tartaglia A., Furton K. G., Locatelli M., Samanidou V. F., *Anal. Methods*, **2019**, *11*(48), 6136
[31] Villar-Navarro M., Moreno-Carballo M. D. C., Fernández-Torres R., Callejón-Mochón M., Bello-López M. Á., *Anal. Bioanal. Chem.*, **2016**, *408*(6), 1615